Biogeochemistry (2011) 102:167–181
DOI 10.1007/s10533-010-9429-2

The influence of phototrophic benthic biofilms on Cd, Cu, Ni, and Pb transport in permeable sediments

Aaron J. Beck · Felix Janssen · Dirk de Beer

Received: 20 August 2009 / Accepted: 8 March 2010 / Published online: 6 April 2010

Abstract The effect of phototrophic biofilm activity on advective transport of cadmium (Cd), copper (Cu), nickel (Ni), and lead (Pb) in sandy sediments was examined using percolated columns. Cd and Ni in the effluent exhibited clear diel cycles in biofilm-containing columns, with concentrations at the end of dark periods exceeding those during illumination by up to 4.5- and 10-fold for Ni and Cd, respectively. Similar cycles were not observed for Pb or Cu. Breakthrough of the latter metals was greatly retarded and incomplete relative to Cd and Ni, and trends in biofilm treatments did not differ greatly from those in control columns. Inhibition of photosystem II by DCMU (3-(3,4-dichlorophenyl)-1,1-dimethylurea) proved that diel cycles of Cd and Ni were controlled by oxygenic photosynthesis, and microsensor measurements showed that metal cycles closely matched metabolic activity-driven pH variations. The sorption edge pH for the sand/biofilm substrate followed the order Ni > Cd > Cu > Pb, and for Ni and Cd, was within the pH 7–10 range observed in the biofilm-containing column. Adsorption dynamics over the light periods matched pH increases, but desorption during dark periods was incomplete and slower than the rate of change of pH. Over a diel cycle, desorption was less than adsorption, resulting in net binding of dissolved metals due to the biofilm metabolic activity. Extraction with selective reagents indicated that the adsorbed metals were readily exchangeable, and potentially bioavailable. Thus, phototrophic benthic biofilms can control the transport of some metals across the sand–water interface, and processes in this very thin surficial layer should be considered when evaluating chemical fluxes in permeable sediments.

Keywords Benthic biofilm · Permeable sediments · Trace metals · Diel cycles · Advection · Submarine groundwater discharge · Subterranean estuary

A. J. Beck · F. Janssen · D. de Beer
Microsensor Group, Max-Planck-Institute for Marine Microbiology, Celsiustrasse 1, 28359 Bremen, Germany

A. J. Beck (✉)
Virginia Institute of Marine Science, College of William and Mary, Gloucester Point, VA 23062, USA
e-mail: abeck@vims.edu

Introduction

Porewater advection dominates transport processes in permeable sediments of both fresh and marine environments (Riedl et al. 1972, Thibodeaux and Boyle 1987, Shaw and Prepas 1990). Such transport allows rapid exchange of dissolved and particulate constituents between water column and sediment, at rates determined by the magnitude of driving forces and sediment permeability (Berner 1980, Huettel et al. 1996, Kloep and Röske 2004). In lakes and rivers, the upper sediment zone containing a mixture

of ground and surface waters is referred to as the "hyporheic zone" (Triska et al. 1993), and magnitude and direction of flow is dominated by surface water flow velocity and groundwater hydraulic pressure (Mutz and Rohde 2003). Advective porewater flow in coastal marine sands is driven by numerous mechanisms, from seawater circulation through the sands by pressure gradients from wave action and currents flowing along sediment surface topography to discharge of fresh groundwater along the coast (Burnett et al. 2003). Cross-interface advective flow in fresh and marine environments is geochemically important both into and out of the sediment, the former bringing reactants such as oxygen and organic matter into the sediment, and the latter flushing metabolic byproducts and sediment leachate into the overlying water (Ehrenhauss et al. 2004; Precht et al. 2004). Advective flux of some chemical constituents can occur in either direction, depending on the site-specific dominance of different processes occurring in the sediments such as metal oxide precipitation (Fuller and Harvey 2000) or dissolution (Huettel et al. 1998).

Chemical flux across the sand–water interface can be greatly affected by the presence and activity of surficial microbial biofilms, and microbial growth can conversely be augmented by advective flow (Battin 2000; Cook and Røy 2006). Phototrophic biofilm activity can completely regulate cross-interface chemical flux by, for example, active assimilation of dissolved Si or passive precipitation of calcite (Woodruff et al. 1999). Passive mechanisms may have particular ecological relevance, as they can affect the geochemical cycling of elements that have little or no physiological function (e.g., Cd), or cause greater fluctuations in concentration than would be caused by biochemical demand alone. In this vein, much recent work has addressed the apparent role of aquatic photosynthesis on diel cycling of arsenate (Fuller and Davis 1989) and trace metals such as Zn, Cd, Mn, and Ni (Nimick et al. 2003, Morris et al. 2006) in circumneutral-pH freshwater streams. In systems where photosynthetic activity is sufficiently high, pH varies as a result of carbon dioxide (CO_2) uptake and release during photosynthesis and respiration, causing diurnal variation in sorption of dissolved metal constituents (Morris and Meyer 2007, Beck et al. 2009). There is further evidence that the large magnitude of pH cycles within phototrophic biofilms causes substantial diurnal metal uptake within the biofilm matrix even in cases where there is little variation in the overlying water column (Morris 2005).

It can be expected that biofilms growing at the sand–water interface exert enormous influence on fluxes of dissolved trace metals across this boundary, but few data are available that demonstrate this effect. Following this hypothesis, we examined the role of photosynthetic benthic biofilms on regulating metal transport in sands. We focused our observations on a selection of heavy metals that differ in geochemical behavior (Ni, Cu, Cd, and Pb).

Materials and methods

Column setup

Flow-through columns (54 mm inner diam.) were constructed of plastic components and designed to provide a constant rate of spatially-homogeneous flow through biofilm covered sands (Fig. 1). Dry sand (37 g) was poured into a water-filled column to prevent bubble trapping, and the column was tapped gently until no further sand compaction was observed (i.e., no

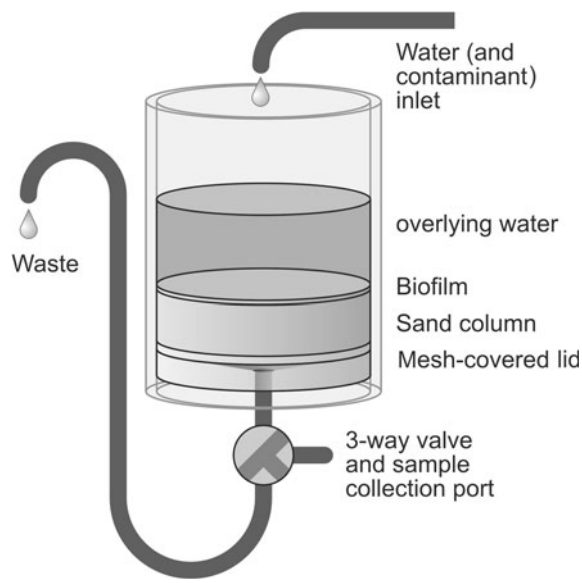

Fig. 1 Flow-though column setup. Metal-spiked water is added to the water column, flows through the biofilm and sand layer, and discharges to waste reservoir. The unrestricted, elevated outlet maintains a constant flow rate that matches the inlet flow

visible decrease in sand column length). This resulted in a homogeneous sand column 1 cm deep. Most experiments were conducted using clean silicate sands (grain size 150–200 μm, permeability $k = 1.5 \times 10^{-11}$ m^2, porosity $\phi = 0.42$), and one experiment (Experiment 3) used sieved (<1000 μm, permeability $k = 5.1 \times 10^{-11}$ m^2) sands collected from the Riou Mort (France). Both were autoclaved and rinsed before use, but experiments were performed under non-sterile conditions. The overlying water in the columns was gently stirred and mixed during the experiments with a low-velocity stream of air blowing on the water surface. White fluorescent lights (photosynthetically active radiation: ~250 μmol photons m^{-2} s^{-1}; OSRAM FQ 80 W/865 HO Lumilux cool daylight) were automatically timed to alternate 12 h periods of light and dark.

A total of four column experiments were conducted using various combinations of biofilm biomass, photosynthesis inhibition, and sand substrate type (see below and Table 1). Biofilms were added to the appropriate columns from an assemblage of green microalgae collected from the metal-contaminated Riou Mort in April 2007, and grown in non-sterile culture since the time of collection (Bold's Basal Medium, metal content unchanged from original recipe; Stein 1973). Algal cells were separated from culture medium by centrifugation, washed twice with clean mineral water to remove residual EDTA-containing medium, and evenly distributed across the sand column surface with a syringe. This did not affect algal activity, and provided a visually uniform, reproducible green biofilm over the sediment surface. Biofilm biomass was adjusted by varying the amount of algal addition to each column; each addition comprised approximately 500 mg of dry algal biomass (thus, a biofilm of "2×" size represented a column algal biomass of ~1 g). Biofilm thickness was 0.5–1 mm, with algal cells tending to disperse among sand grains in the upper 1 mm instead of forming a discrete layer at the very surface. Algae were added to the columns approximately 2 days before the start of metal addition. No substantial change in biofilm appearance was visually evident over the course of the experiments, indicating little growth or deterioration. Control columns were constructed as in biofilm treatments, but omitted the algae addition.

Samples were collected at the outlet of the column directly into 2 ml acid-washed polyethylene microcentrifuge tubes, except for the 48 h time series, when samples were collected continuously over 1 h intervals using a multi-channel syringe pump connected to the outlet valve. Comparison of unfiltered and filtered (0.22 μm, nylon) column effluents during column experiment 1 showed little or no difference (<10%), so simple unfiltered samples were collected in subsequent experiments.

The columns were percolated with dilute metal solutions (2–3 μM Cd, Cu, Ni, Pb, pH ~7) made from concentrated (1 g l^{-1}) ICP standard solutions (TraceCERT, Fluka, Switzerland) in bottled, still mineral water (Aldi) with no nutrients or reduced carbon substrate added. Metal solution flow into each column was regulated by a peristaltic pump at 4.8 ml h^{-1}, or ~0.5 cm h^{-1} (cm^3 cm^{-2} h^{-1}). DCMU (3-(3,4-dichlorophenyl)-1,1-dimethylurea) was dissolved in 200 μl methanol and added to the metal solution of one column (10 μM final concentration) to inhibit photosynthesis (Tomaselli et al. 2002). Breakthrough of an inert tracer

Table 1 Description of column experiments

Column experiment number and description	Experimental treatments	Duration (days)	Substrate type[a]	Phases sampled	Sampling frequency
1. Biofilm and diel cycle	Control; 1× and 3× biofilm biomass; DCMU-inhibited biofilm	6	Clean sand	Effluent water, sands	2 day^{-1}, end of light and dark periods
2. Biofilm biomass	Control; 1×, 2× and 5× biofilm biomass	3	Clean sand	Effluent water	2 day^{-1}, 7× during one light period
3. Natural sands	Control; 1× biofilm biomass; DCMU-inhibited biofilm	8	Natural sand	Effluent water, sands	2 day^{-1}, end of light and dark periods
4. 48 h time series	Control, 1× biofilm biomass	7 + 3	Clean sand	Effluent water	Hourly for 48 h

[a] See text for details on sand characteristics

(17 mM NaCl) was monitored in one column with a conductivity sensor placed at the column outlet.

All column experiments were performed in a temperature controlled room at 15°C. Metal concentrations were determined by ICP-OES (plasma-source optical emission spectrometry) on a Perkin-Elmer Optima 3300RL. A standard reference material (NIST 1643e—Trace Elements in Water) was used to confirm that the instrument accuracy was within ±10% of certified values. Instrument precision was generally better than 5% for all elements.

Oxygen and pH measurements

Oxygen and pH profiles were measured in the upper 5 mm of the sand columns using needle-type microsensors (Gieseke and de Beer 2004). Oxygen was measured using a Clark-type microelectrode with guard cathode (~150 μm tip diameter; Revsbech and Jørgensen 1986) connected to a pA meter. The sensor was calibrated in air- and N_2-purged water. pH was measured using a LIX (liquid ion exchange) microelectrode (tip diam. ~100 μm) connected to a mV meter, and calibrated with pH 7 and 9.15 buffer solutions (Gieseke and de Beer 2004). Electrodes were mounted on a micromanipulator attached to a motorized linear drive (Faulhaber), affording ~1 μm vertical positioning precision. Analog signals from the microelectrodes were digitized and recorded with a data acquisition device (DAQ 6015, National Instruments) connected to a computer. Microprofiling was automated using the μ-Profiler software (Garching Innovation GmbH, developed by L. Polerecky, MPI-Bremen).

Sediment leaches

Following completion of the effluent sampling, columns were drained, and the sands excavated at 2 mm intervals to 6 mm depth. These sand samples were then freeze-dried and homogenized. Aliquots of 1 g were subjected to parallel leaching with four different reagents to assess metal partitioning among different sediment phases. Parallel extractions were used because non-specificity of the treatments can lead to under-estimation of the later fractions during sequential extractions (Martin et al. 1987, Tessier and Campbell 1991). Dilute acetic acid (0.11 M) was used to determine the labile, easily exchangeable fraction (Davidson et al. 1998), hydroxylamine hydrochloride (0.5 M) to access the reducible (metal-hydroxide) phase (Rauret et al. 1999), hydrogen peroxide (8.8 M) to digest organic matter (Rauret et al. 1999), and concentrated aqua regia to leach the residual metal fraction (Davidson et al. 1998). The aqua regia leach did not completely dissolve the silica sand matrix. Reagents were added to dried sediments and allowed to react for 24 h on a shaker table. The leaches were then centrifuged (Quevauviller et al. 1993), decanted, and the supernatant acidified to pH <2 with ultrapure HNO_3. The peroxide treatment was UV-irradiated for 24 h after acidification to decompose excess H_2O_2.

pH experiment

The pH dependence of metal sorption onto clean sand (1 g dry wt.) and clean sand (1 g dry wt.) plus algal inoculum (11 mg dry wt.) was determined as described in Beck et al. (2009). These solid substrates were equilibrated with 5 μM metal-spiked mineral water, and pH was adjusted to span the range pH 2–12 using 0.1 M solutions of HCl and NaOH. After 1 h, samples were syringe-filtered (0.45 μm, nylon), and were acidified to pH <2 with ultrapure HNO_3 before analysis.

Results and discussion

Column experiment 1: biofilms and diel metal cycles in clean sand columns

Individual metal geochemistry greatly affected transport through the sands, as breakthrough of all four metals in biofilm-free control sand columns was substantially different from that of the inert NaCl tracer and each other (Fig. 2). Breakthrough of the inert tracer was observed after 2 h, consistent with the set flow rate. The tracer showed that approximately 12 h were required to completely replace both overlying water and porewater and reach steady state between inflow and outflow concentrations. In contrast, Ni and Cd concentrations reached steady state only after approximately 3 days (Fig. 2), suggesting substantial adsorption of the dissolved metals to sand surfaces during initial stages of the experiment. Effluent Pb and Cu concentrations reached only 30% of the inlet concentrations after 1 week. The marked

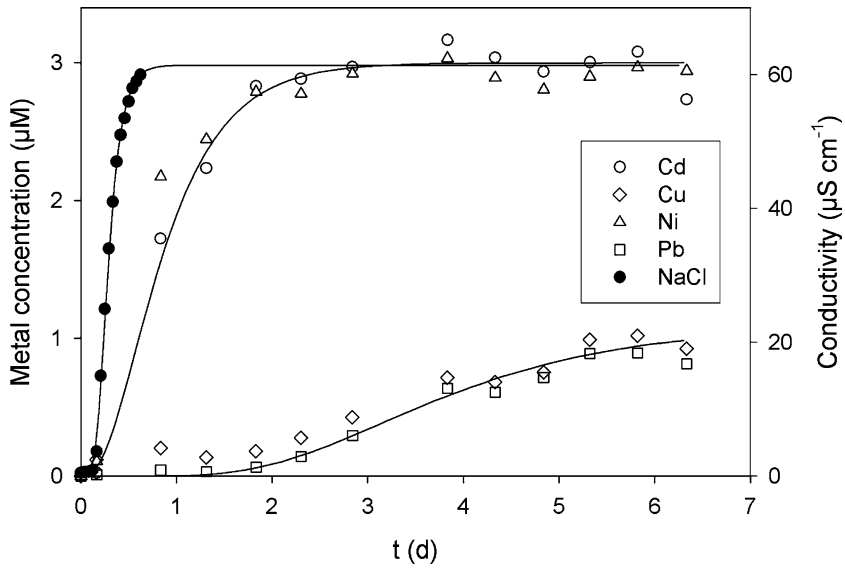

Fig. 2 Inert tracer (NaCl, measured as conductivity) and control treatments. Metal data are from column experiment 1 (see *text*), and tracer data are from a separate test. *Curves* are drawn through constituents with similar trends to guide the eye: NaCl, Ni/Cd, and Cu/Pb

retention of Pb and Cu in the sand columns is consistent with their greater tendency for adsorption to surfaces (Langmuir 1997).

Striking diurnal variations of Ni and Cd concentrations in the outflow were observed in columns with active photosynthetic biofilms (Fig. 3), while no similar patterns were evident for Pb or Cu. Effluent metal concentrations at the end of the dark periods represented an increase over day by 4.5-fold and 10-fold compared to concentrations at the end of the day for Ni and Cd, respectively. The diel cycles observed for Ni and Cd clearly resulted from photosynthetic activity in the biofilm, as inhibition of photosynthesis with DCMU resulted in trends that almost exactly matched the control (no biofilm) treatment (Fig. 3). Effluent concentrations in the DCMU treatment were slightly lower than in the control, likely resulting from the additional sorption sites associated with the microalgae. Photosynthetic control of the metal cycles is consistent with previous studies showing that pH variations driven by CO_2 uptake and release can regulate metal sorption in circumneutral-pH freshwater systems (e.g., Fuller and Davis 1989, Morris et al. 2005, Beck et al. 2009). Given the controlled conditions of the current study, we can neglect influences of temperature, other metal sources, and photochemical or precipitation reactions of Fe and Mn (cf. Nimick et al. 2003).

There was a clear effect of biofilm biomass on the magnitude of the diel cycles, with a 3-fold increase of algae biomass resulting in much lower effluent dissolved metal minima [e.g., 2.5 vs. 1.0 µM (1× vs. 3× minima) and 2.6 vs. 1.7 µM for Cd and Ni, respectively; Fig. 3]. Although no diel cycles were observed for Pb or Cu, biomass seemed to retard transport of these metals as well, most likely due to an increase in available surface sorption sites, as discussed below.

pH experiment

The striking difference in behavior between the more weakly adsorbed Ni and Cd and strongly adsorbed Cu and Pb highlights the importance of individual metal geochemistry to the cyclic diel pattern. Figure 4 shows the influence of pH on metal sorption to sand and mixed sand-biofilm substrates. The experimental data show exactly the differences in pH-dependence between metals that would be expected for a given substrate (e.g., hydrous ferric oxides; Dzomback and Morel 1990), with the pH of the sorption edge (i.e., 50% adsorbed) varying in the order Ni > Cd > Cu > Pb (pH values of 8.45, 7.28, 5.48, and 4.75, respectively). It is doubtless that the pH of the sorption edge of these curves (though probably not the order) will vary depending on the zero point of charge (ZPC) of specific substrates (Langmuir 1997). Indeed, the sorption edge for the sand/algae mixture was centered at a slightly more acidic pH than the sand alone, consistent with the tendency of algal cells to change the response of the

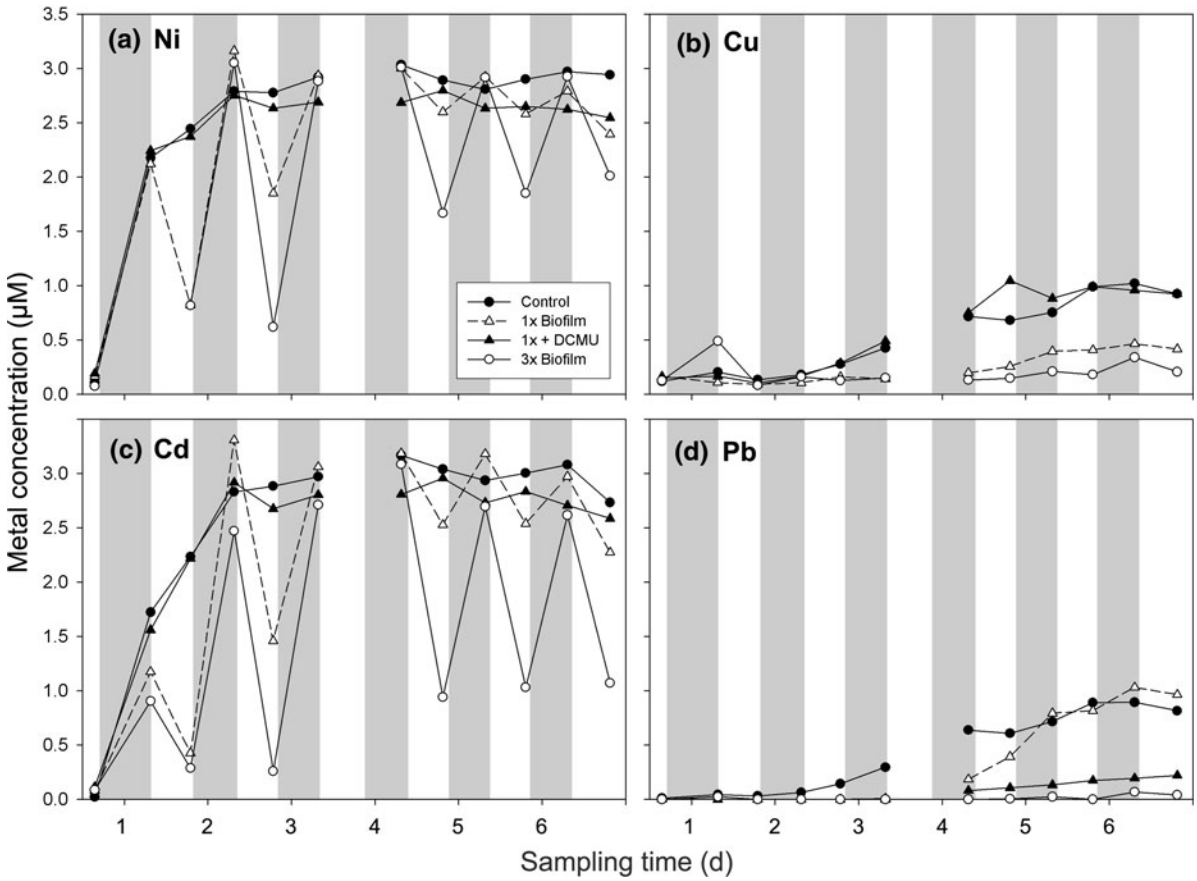

Fig. 3 Trace metal concentration in column effluent in experiment 1. Control data are the same as those shown in Fig. 2. *Shaded areas* represent dark periods. **a** Ni, **b** Cu, **c** Cd, **d** Pb. The sample from the point before day 4 was not collected

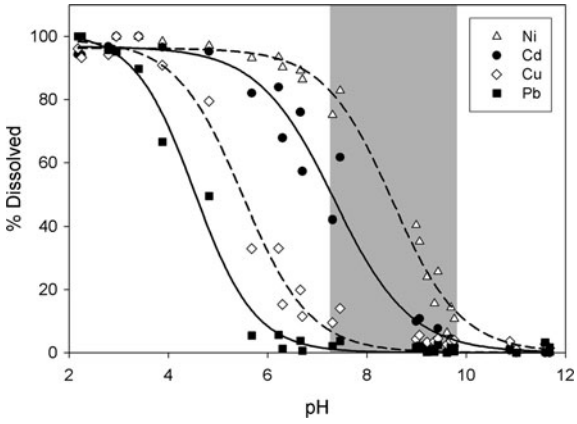

Fig. 4 pH sorption experiment. Data indicate the amount of added metal remaining in solution after equilibration at different pH values. *Lines* are drawn to guide the eye, and represent fits of the data for each metal. The *shaded area* represents the range of pH measured in the sediment column during experiment 2. Cd data from Beck et al. (2009)

system to changes in proton concentration (Gonzalez-Davila 1995). However, the difference between metals was much greater than the difference for a single metal between sorbents, and data from both sorbent types are combined in Fig. 4.

Column experiment 2: biofilm biomass influence on diel cycles

It was shown previously (Beck et al. 2009) that Cd diel variation can be explained by photosynthesis- and respiration-driven pH cycles that encompass the Cd sorption edge. From the pH experiment, it seems likely that this explanation holds for the other metals as well, with pH in the biofilm columns decreasing sufficiently to mobilize Ni, but not Cu or Pb. To confirm this, a second column experiment was conducted with different amounts of biofilm biomass,

and pH and O_2 in the biofilm were measured with microsensors.

The results again showed significant diel cycles for Ni and Cd (Fig. 5), but not for Pb or Cu (data not shown). There were marked differences between different biofilm sizes, with the two least dense biofilms initially showing the largest concentration changes. For Ni, in the most dense biofilm treatment, effluent concentrations approached the maximum more slowly, but the cycles became increasingly large and eventually exceeded the other two treatments. For Cd, substantial breakthrough was not observed in the densest biofilm treatment over the 3-day experiment, indicating an overabundance of sorption sites for the short experiment duration. An interesting feature of the Ni trends is that maximum effluent concentrations were similar among the three treatments, and within ±10–20% of the control (1.90–2.17 μM; Fig. 5). However, the minimum metal concentrations at the end of the experiment (1.05 μM for 1×biofilm, and 0.18 μM for 3× biofilm; Fig. 5) differed substantially between treatments and approximately proportionally to the size of the biofilm inoculum. This agrees with observations from the first column experiment (Fig. 3).

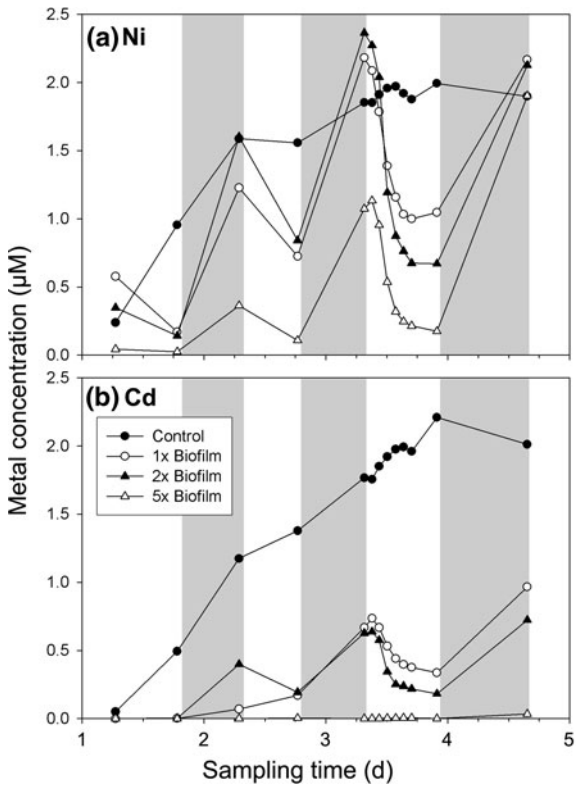

Fig. 5 **a** Ni and **b** Cd concentrations at the column outlet of the biofilm biomass experiment (column experiment 2). *Shaded areas* represent dark periods

Oxygen and pH microprofiles showed that ranges of both parameters in the three biofilm treatments generally scaled with the size of the biofilm inoculum (Fig. 6). pH values increased greatly during the day, reaching maxima of 8.7, 9.1, and 9.7 in the 1×, 2×, and 5× biofilm treatments, respectively. Likewise, oxygen concentrations increased to 515, 676, and 818 μM in the 1×, 2×, and 5× treatments, respectively. The decreases in dark periods were less pronounced in the 1×, 2×, and 3× treatments, reaching minimum pH values of 7.7, 7.3, and 7.4, respectively, and oxygen concentrations of 280, 266, and 245 μM, respectively. In the control column, only small differences between light and dark periods were observed for both pH (0.1 unit) and oxygen (7 μM).

At a given flow rate, biofilm metabolic activity resulted in steady-state oxygen concentrations (and thus, CO_2 concentrations and pH) that were roughly proportional to biofilm biomass. Therefore, the similar metal effluent concentrations observed at the end of the dark period resulted from similar pH values at that time, while the greater differences in concentration during daytime were a consequence of the large differences in pH between the three biofilm treatments (Figs. 5, 6). In addition, it seems that when CO_2 uptake (O_2 production) and advective flow supply achieved a steady-state pH, a particular equilibrium metal concentration in the effluent also resulted, consistent with previous reports of pH-dependent metal sorption (Padmanabham 1983). This is clearly evident in the plateau behavior of the metal curves (minima) during the light period (Fig. 5). Lastly, comparing the range of pH measured in the second column experiment (Fig. 6) with the trends observed in the pH-sorption experiment (Fig. 4), it is obvious that Cd and Ni would be expected to vary between highly mobile at the lowest measured column pH and highly immobile at the highest measured pH. In contrast, the sorption edge of both Pb and Cu is centered at a lower pH than the minimum measured in the column experiment. Less than 20% of Cu and 5% of Pb would be expected to remain in the dissolved phase even at the very lowest pH levels observed in

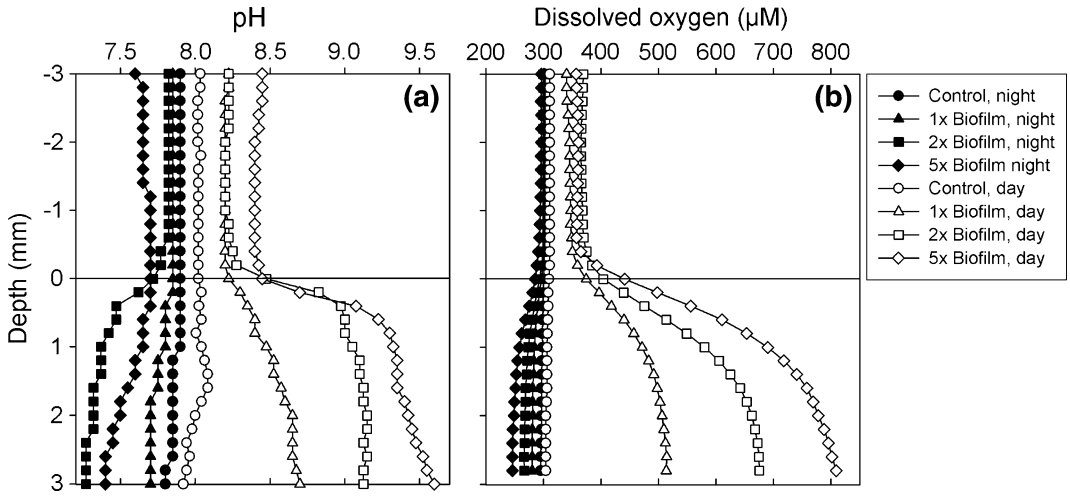

Fig. 6 Microprofiles of **a** pH and **b** O_2 from the biofilm biomass experiment (column experiment 2), measured on day 4. Positive depths indicate distance into the sediment, and the *horizontal line* indicates the position of the sediment surface. Algal cells of the biofilm were dispersed with sand grains and generally populated the upper 1–2 mm

the biofilm, and thus, no diel cycle is observed. It is worth noting that although we did not examine Zn in the current study, its position relative to the sorption edge of other metals in Fig. 4 would be between Ni and Cd (Stumm and Morgan 1996), and we would predict that Zn should also show a diel cycle under our experimental conditions. This is consistent with the numerous studies that report clear Zn cycles in contaminated freshwater streams (e.g., Nimick et al. 2003, and references therein).

Column experiment 3: natural sand substrate

From the greater metal retention of Cd and Ni in the DCMU treatment relative to the control column (Fig. 3) and at high relative to low biofilm density (Fig. 5), it is obvious that substrate composition has a profound effect on the sorption of these metals. We replicated the first column experiment, but used instead natural sands containing high levels of acid leachable Fe (1.7%) and Mn (0.07%), presumably present as (hydr)oxide surface coatings. Over the 8-day experiment duration, none of the 4 metals examined was found in any of the column effluents (data not shown). It is clear from this finding that although the pH-dependent sorption characteristics of this natural sand did not differ greatly from the clean experimental sands (as shown for Cd; Beck et al. 2009), the natural sands had a much higher capacity for metal adsorption and retention. A diel cycle would not be detectable until the strong (irreversible) sorption sites are saturated. The metal distribution in the column sands confirms that retention in the natural sands was higher than the clean sands (discussed below).

Column experiment 4: high-resolution 48 h time series

To more fully examine the kinetics of diel cycles observed in the clean sand columns, we performed a fourth, higher-resolution column experiment with clean sands. Guided by the first experiment, we waited one week to allow cycles to reach approximate steady state, and then performed hourly sampling of the effluent for a 48 h period. As expected from prior experiments, Pb and Cu showed limited breakthrough and no diel cycle (data not shown). Ni followed a smooth diel cycle that reached inlet concentrations, but unfortunately, the biofilm was too dense, and as in the second column experiment, only a small degree (0.025 μM, or 1% of the inlet concentration) of Cd breakthrough occurred (Fig. 7). Nonetheless, even these very low Cd concentrations exhibited a clear diel cycle, although there is more scatter in the data due to the limited sensitivity of the ICP-OES measurement technique. Consequently, we will focus our discussion on Ni, and we expect that Cd is subject to the same controlling mechanisms as Ni.

A striking feature of the Ni time series is that the increase during the dark periods occurred nearly

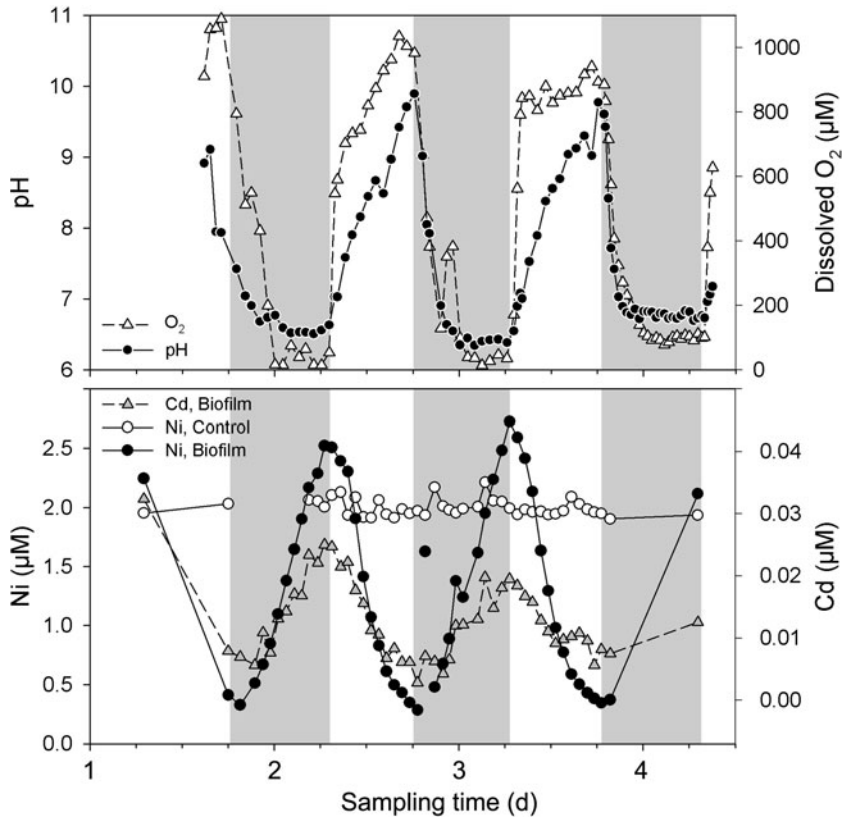

Fig. 7 48 h time series experiment (column experiment 4). *Upper panel* shows pH and O_2 time series at 4 mm depth extracted from microsensor profiles. *Lower panel* shows metal concentrations in effluent water. Note the different scales for Cd (*right-hand*) and Ni (*left-hand*). *Shaded areas* represent dark periods

linearly, while the decrease during light periods followed a sigmoidal trend (Fig. 7). The Ni concentration plateau observed at the end of the light period (Fig. 7) is in agreement with the results of the second column experiment (Fig. 5). The difference in Ni behavior between light and dark periods was mirrored by starkly contrasting light and dark pH trends (pH from 4 mm depth in the columns, Fig. 7). While dissolved O_2 displayed large and immediate changes at the beginning of both light and dark periods, pH increased much more slowly (0.29 ± 0.01 units h^{-1}) than it decreased (1.1 ± 0.2 units h^{-1}).

Interestingly, this resulted in establishment of a pH plateau late in the dark period, whereas Ni reached its plateau at the end of the light period (Fig. 7), and the two appear to have been disconnected. To explore this pattern further, Fig. 8 plots Ni in the column effluent against pH, with the data distinguished by sampling time. The data appear to form a loop, and there is clear hysteresis in the Ni response to changes in pH. As pH increased after illumination began, Ni and pH exhibited an apparently sigmoidal covariation. This resulted in a slight plateau at pH values <7 and >9. After the light was switched off, pH decreased rapidly, and faster than Ni responded. Once pH was below ~7, Ni slowly began to increase to maximum concentrations. While the observed hysteresis may potentially have been exaggerated by the flow through delay in the column (i.e., because of the separation between water inlet, biofilm, and water outlet), this probably explains only a small portion of the observed pattern. The Ni trends of decrease and increase are clearly delimited by the light–dark timing. The inert tracer data showed that only about 6–8 h were required to flush >90% of the column (Fig. 2), but changes in metal concentrations occurred over at least a 12 h period (Fig. 7).

If we normalize the maximum Ni concentrations from the column experiment to 100% and plot the data from the light periods of the 48 h time series on the curves from the pH-sorption experiment in Fig. 4, it is evident that the observed sigmoidal pattern matches very well with the pH-dependent Ni sorption behavior (Fig. 8), and is clearly distinct from the adjacent Cd curve. The non-zero plateau observed for Ni in the effluent at high pH is likely due to complex

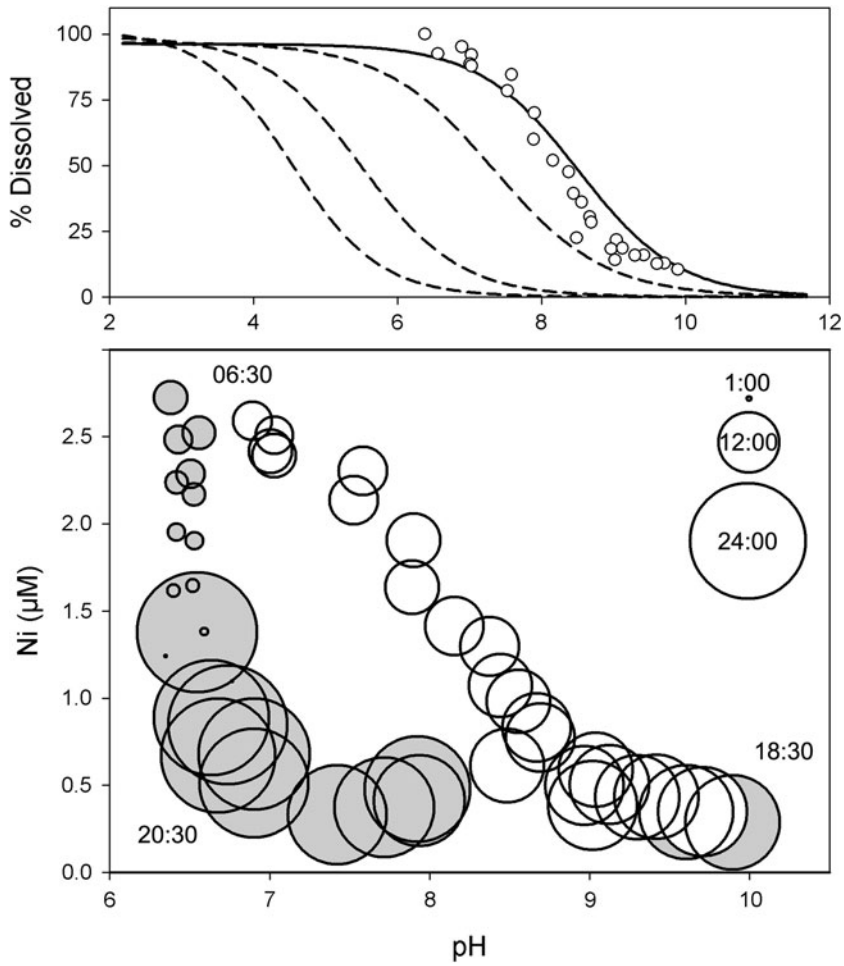

Fig. 8 48 h time series (column experiment 4). *Upper panel* shows the curves from Fig. 4 overlain with the Ni concentration data in the column effluent from light periods of the 48 h time series experiment. *Lower panel* shows Ni concentrations in the effluent plotted against pH, where the *symbol* size indicates time of day. Dark periods are indicated by the *shaded circles*. The timing of the vertices is indicated

formation with biofilm-produced soluble ligands (Gonzalez-Davila 1995).

It is clear that sorption processes play a major and probably dominant role in causing the metal–pH hysteresis. The Ni–pH pattern during the day closely matched the experimental pH-dependent sorption trends, suggesting that Ni adsorption in the column is comparable to or faster than the rate of change of pH. During pH decrease, Ni desorption is both incomplete and slower than the rate of change of pH. This is consistent with previous reports of hysteresis in heavy metal adsorption–desorption reactions (Maes and Cremers 1975; Strawn et al. 1998). The approximately 30% increase in maximum effluent concentrations in the biofilm treatment relative to the control indicates that a substantial amount of Ni is desorbed from the sands. Thus, in addition to regulating adsorption (flux reduction vs. constant flux), the biofilm also affects desorption (flux increase). At steady state, the net flux will be constant, but the diel variation may be ecologically important nonetheless.

Sediment metals distribution

The distribution of sediment-bound metals should reflect and confirm the interpretations of different metal behavior discussed for the aqueous phase above. There was no difference among the different leaches (acetic acid, hydroxylamine HCl, hydrogen peroxide, and aqua regia) of the first experiment sands, indicating that all of the metals adsorbed to the sediment grains were easily exchangeable (data not shown). Similar extraction of the natural, metal oxide rich sands showed large differences among the leaches, particularly in the aqua regia treatment

(discussed below). In order to have a consistent comparison between sediment types, and because the acetic acid leach reflects the readily exchangeable, potentially bioavailable metal fraction, it is the only treatment that will be discussed here.

There were clear differences among the acetic acid extractible metal profiles in the upper 6 mm of the sediment columns (Fig. 9). In the control column, there was sharp contrast between the Ni and Cd profiles and those for Cu and Pb. Both Ni and Cd showed constant concentrations with depth, whereas Pb and Cu showed decreases. This is consistent with the requirement that sorption sites for each metal be nearly saturated before significant breakthrough will be observed in the column effluent. The constant Ni and Cd content with depth indicates that they reached a sorption maximum in the control column sediments (Fig. 9). This agrees with the observation that Cd and Ni in the effluent reached steady state with respect to the inlet concentrations after 2–3 days (Fig. 2). In contrast, decreasing levels of Cu and Pb with depth in the control sands (Fig. 9) indicate that not all sorption sites had been occupied by the end of the experiment, and that limited dissolved metal would be expected in the effluent water. Indeed, this is evident in the highly retarded breakthrough trends for Cu and Pb (Fig. 2).

For all four metals, the surface layer in the biofilm columns, both with and without DCMU, showed pronounced enrichment relative to deeper layers, confirming that there was substantial metal sorption to the algae (Fig. 9). Biofilm and DCMU columns show similar mid and bottom depth concentrations for Cd and Ni, and concentrations that decline slightly with depth for Pb and Cu. This suggests that sorption sites were saturated at these depths for Cd and Ni, but not for Pb or Cu. However, it is not clear why the concentrations differ so greatly between these two treatments, especially for Ni (Fig. 9).

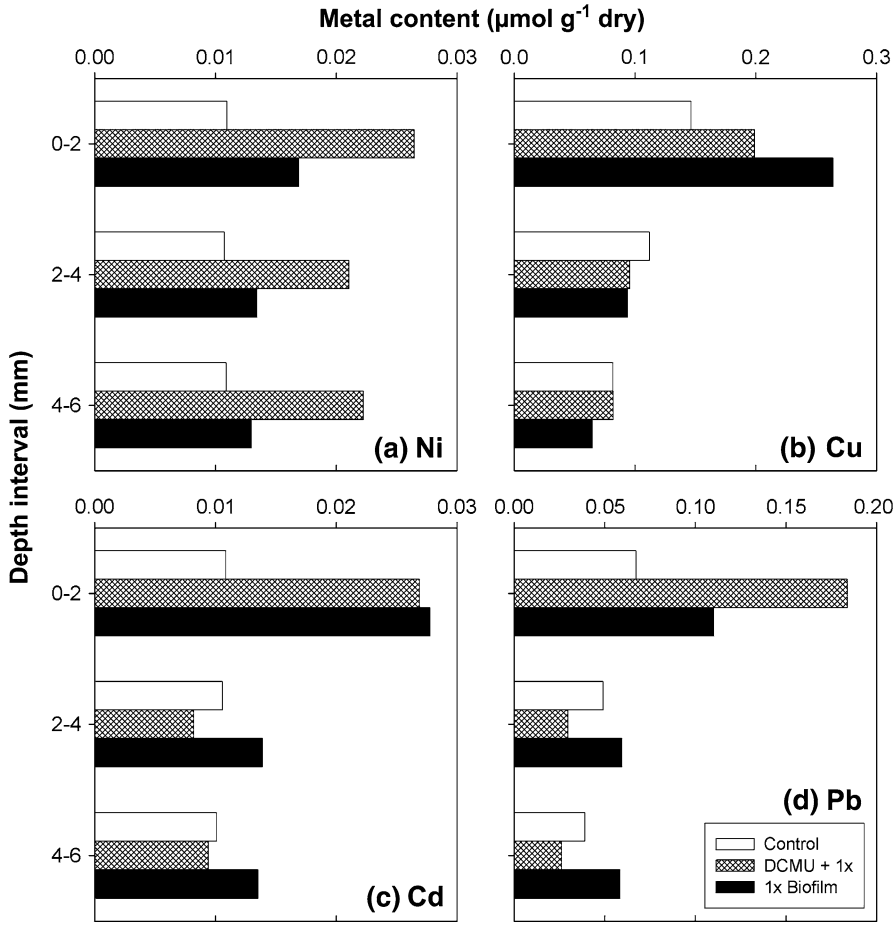

Fig. 9 Acetic acid extractable metals in sands from column experiment 1 (clean sands). Note the different *x*-axis scales. **a** Ni, **b** Cu, **c** Cd, **d** Pb

The DCMU treatment should have had sedimentary metal inventories that were higher than the controls (due to sorption on algal cells), but lower than the biofilm treatment (due to light period sorption dominating over dark period desorption). This was only evident for Cd and Cu; the biofilm treatment Pb inventory was only slightly less than the DCMU treatment, but the difference was very large for Ni. The cause of this is not obvious, although the effluent data (Fig. 3) indicate that during dark periods, the Ni concentration was indeed higher in the biofilm treatment than in the DCMU treatment (by $\sim$10%).

It does not appear that this difference was sufficient to account for the very large mismatch in sediment inventories (the Ni inventory in the DCMU treatment was higher than the biofilm treatment by $\sim$50%), but the effluent data are too coarse to be conclusive. As the biomass experiment (Fig. 5) and the 48 h time series experiment (Fig. 7) showed, concentration increases and decreases were not necessarily linear or symmetric. Additionally, differences in algal biomass may also have been present between the two treatments, with greater biomass in the DCMU treated column leading to higher adsorption capacity. It may further be possible that the adsorption affinity of individual metals for algal cells is different for actively photosynthesizing cells than inactive ones.

Compared to the clean sands, the natural sands were enormously enriched in Fe and Mn, by 200-fold and 1300-fold, respectively, making the natural sands a much more powerfully adsorbing substrate (Benjamin and Leckie 1981). This is clearly evident in the sharply and continuously decreasing sediment metal profiles from the natural sand experiment (Fig. 10). Most of the metal is apparently extracted from solution onto the sands in the uppermost 2 mm of the column. In natural systems, it is likely that sorption onto such highly reactive surfaces as Fe- or Mn-oxides will dominate metal cycling until the sorption sites are

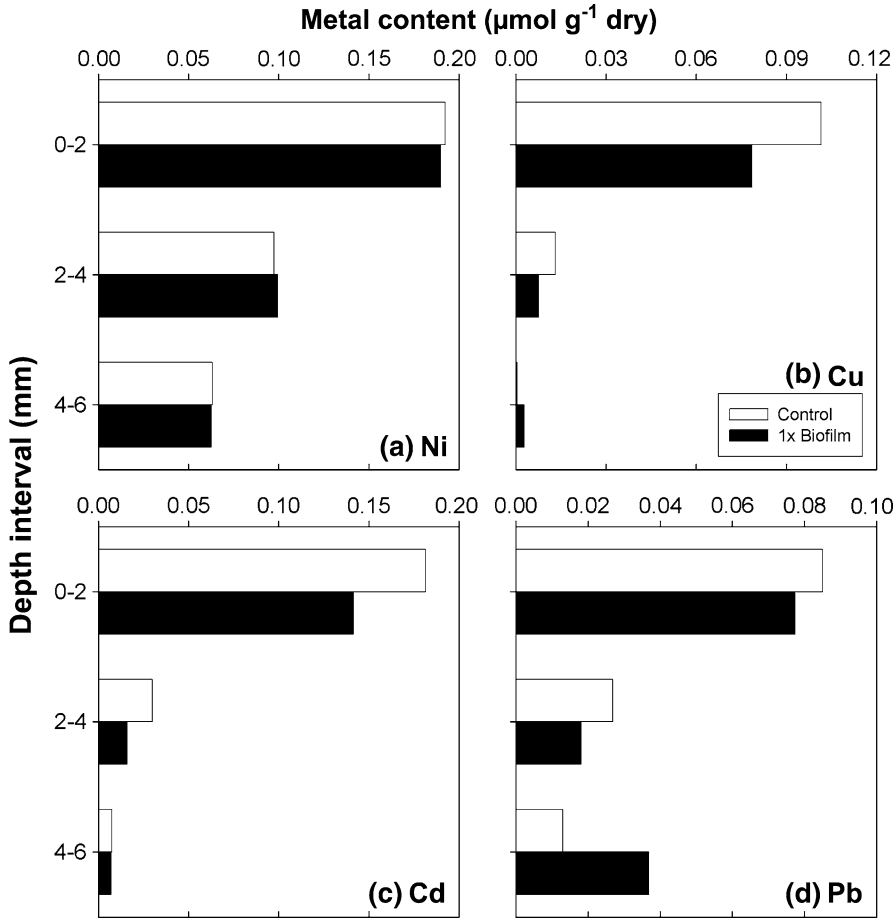

Fig. 10 Acetic acid extractible metals in sands from column experiment 3 (natural sands from Riou Mort). Note the different *x*-axis scales. **a** Ni, **b** Cu, **c** Cd, **d** Pb

saturated and equilibrium is reached. This is in agreement with the findings of Fuller and Harvey (2000), who showed that dissolved metals in a stream decreased along the flowpath due to scavenging on authigenic Mn-oxides in the hyporheic zone. In systems where ongoing processes such as Mn- or Fe-oxide precipitation keep sands from reaching equilibrium or steady state with respect to their cation sorption capacity, it is likely that phototrophic biofilm activity will not be the dominant control on metal cycling. However, the biofilm may play an intermediate role in metal redistribution, e.g., with sorption first to the photosynthesizing, pH-basic biofilm, and subsequent transfer to and trapping on underlying metal oxide crusts (as postulated by Morris 2005).

Implications of biofilm-mediated sorption for metal cycling in the environment

The results of this study suggest that the influence of phototrophic benthic biofilms on metal transport in sands will depend on biofilm density and activity relative to flow rate and composition of the sand substrate. A small biofilm under low flow conditions will likely influence discharging metal concentrations to the same degree as a dense biofilm under high flow conditions. Ultimately, the biofilm effect is due to the ability of the biofilm to change the CO_2 content and pH of the interstitial water. Hence, in addition to the flow rate, factors such as light intensity, heterotroph metabolism/respiration, and buffer capacity of the water and sediments will all affect the degree of pH change and metal partitioning. The composition of the sand itself is also important, and sediments with high cation exchange capacity will suppress diel cycles until sorption sites are nearly in equilibrium with the solution. Processes that keep sands from achieving this equilibrium, such as sediment redistribution and surface metal oxide precipitation, will tend to prevent establishment of diel metal concentration patterns in the exchanging water.

The photosynthesis-driven metal sorption mechanism elucidated in the current study may be difficult to discern in natural systems due to the fact that other processes follow the same diel cycle. For instance, this variable metal sorption in freshwater streams will generally be in phase with diel cycles of hyporheic input caused by evapotranspiration on the shores (Nimick et al. 2003). At night, higher hyporheic discharge will be accompanied by decreased metal retention, and a high metal flux should result. Conversely, daytime low flow and high sorption conditions will produce a combined decreased flux. It may therefore be difficult to differentiate between hydrologic and biologic control on metal cycles in freshwater streams, and the relative importance of each should be considered in systems where both are expected to occur.

Biofilm controlled sorption mechanisms appear to greatly increase the pool of labile, easily exchangeable metals which may be available to deposit feeding macrofauna. Differing metal sorption behavior due to individual geochemistry may cause fractionation of mixed-metal solutions, where, for example, Ni is mobile and transported at a given pH, but Pb is immobilized and sequestered in the sediments. This effect may have implications for toxicology and trophic transfer, as it changes the suite of toxicants to which organisms may be exposed, as well as the route of exposure.

Previous studies have shown clearly that porewater flow in permeable sediments can affect redox zonation and drive metal-enriched porewater into the water column (e.g., Huettel et al. 1998). Our results complement that conclusion by showing that even without anoxic porewater discharge, phototrophic benthic biofilm activity can strongly affect the sequestration and release of some trace metals. Large scale changes in pH commonly occur in phototrophic biofilms, even in well-buffered systems where photosynthesis effects on water column pH are minimal, such as the marine environment. Thus, in most pH-circumneutral environments, water percolating through the "biofilm sieve" will experience much different and more dynamic conditions than exist in either water column or porewater, potentially having a profound effect on metal transport and fate in those systems. Given the high concentrations of metals often found in slightly acidic fresh groundwater (e.g., Coynel et al. 2007; Charette and Sholkovitz 2006), microbenthic photosynthesis may be a dominant factor regulating input of metal contaminants to freshwater and coastal ocean ecosystems. Consequently, accurate estimates of chemical flux from shallow permeable sediments, and subsequent assessment of the ecological relevance of this discharge, may require close monitoring of biofilm activity in the sand surface.

Conclusions

We observed marked diel cycles in effluent metal concentrations from a biofilm-covered sand column. We demonstrated that these cycles were driven entirely by pH-dependent sorption changes as a consequence of CO_2 uptake and release during photosynthesis and respiration. The size of the biofilm and level of metabolic activity exerted substantial control on the degree of pH change, and the subsequent magnitude of dissolved metal sorption. It is evident from these results that photosynthetic biofilms growing at the sand–water interface in natural environmental systems may play a profound role in regulating the exchange of metals between water column and sediment compartments. Because advective transport processes in sandy sediments are important in both fresh and marine ecosystems, phototrophic biofilms may be a major control on metal cycling in all illuminated aquatic sands.

Acknowledgements Funding for this study was provided by the ECODIS project (European Commission's 6th framework program, subpriority 6.3 "Global Change and Ecosystems," under contract 518043). We greatly appreciate assistance with microsensor construction from the Microsensor Group technicians: I. Dohrmann, G. Eickert, K. Hohmann, A. Niclas, I. Schröder, and C. Wiegand. We also wish to thank Silvana Pape (U. Bremen) for ICP-OES assistance. This manuscript benefitted from comments by two anonymous reviewers.

References

Battin TJ (2000) Hydrodynamics is a major determinant of streambed biofilm activity: from the sediment to the reach scale. Limnol Oceanogr 45(6):131–1308

Beck AJ, Janssen F, Polerecky L, Herlory O, de Beer D (2009) Phototrophic biofilm activity and dynamics of Diurnal Cd cycling in a freshwater stream. Environ Sci Technol 43:7245–7251

Benjamin MM, Leckie JO (1981) Multiple-site adsorption of Cd, Cu, Zn, and Pb on amorphous iron hydroxide. J Colloid Interface Sci 79(1):209–221

Berner RA (1980) Early diagenesis: a theoretical approach. Princeton University Press, Princeton, 241 pp

Burnett WC, Bokuniewicz HJ, Huettel M, Moore WS, Taniguchi M (2003) Groundwater and pore water inputs to the coastal zone. Biogeochemistry 66:3–33

Charette MA, Sholkovitz ER (2006) Trace element cycling in a subterranean estuary: part 2. Geochemistry of the pore water. Geochimica et Cosmochimica Acta 70(4):811–826

Cook PLM, Røy H (2006) Advective relief of CO_2 limitation in microphytobenthos in highly productive sandy sediments. Limnol Oceanogr 51(4):1594–1601

Coynel A, Schäfer J, Dabrin A, Girardot N, Blanc G (2007) Groundwater contributions to metal transport in a small river affected by mining and smelting waste. Water Res 41:3420–3428

Davidson CM, Duncan AL, Littlejohn D, Ure AM, Garden LM (1998) A critical evaluation of the three-stage BCR sequential extraction procedure to assess the potential mobility and toxicity of heavy metals in industrially-contaminated land. Anal Chim Acta 363:45–55

Dzomback DA, Morel FMM (1990) Surface complexation modeling: hydrous ferric oxide. Wiley-Interscience, New York

Ehrenhauss S, Witte U, Bühring SI, Huettel M (2004) Effect of advective pore water transport on distribution and degradation of diatoms in permeable North Sea sediments. Mar Ecol Prog Ser 271:99–111

Fuller CC, Davis JA (1989) Influence of coupling sorption and photosynthetic processes on trace-element cycles in natural waters. Nature 340(6228):52–54

Fuller CC, Harvey JW (2000) Reactive uptake of trace metals in the hyporheic zone of a mining-contaminated stream, Pinal Creek. Ariz Environ Sci Technol 34:1150–1155

Gieseke A, de Beer D (2004) Use of microelectrodes to measure in situ microbial activities in biofilms, sediments, and microbial mats. In: Kowalchuk GA, de Bruijn FJ, Head IM, Akkermans AD, van Elsas JD (eds) Molecular microbial ecology manual. Kluwer, Dordrecht, pp 1581–1612

Gonzalez-Davila M (1995) The role of phytoplankton cells on the control of heavy metal concentration in seawater. Mar Chem 48:215–236

Huettel M, Ziebis W, Forster S (1996) Flow-induced uptake of particulate matter in permeable sediments. Limnol Oceanogr 41(2):309–322

Huettel M, Ziebis W, Forster S, Luther GW III (1998) Advective transport affecting metal and nutrient distributions and interfacial fluxes in permeable sediments. Geochim Cosmochim Acta 62(4):613–631

Kloep F, Röske I (2004) Transport of algal cells in hyporheic sediments of the River Elbe (Germany). Int Rev Hydrobiol 89:88–101

Langmuir D (1997) Aqueous environmental geochemistry. Prentice-Hall, New Jersey

Maes A, Cremers A (1975) Cation exchange hysteresis in montmorillonite a pH-dependent effect. Soil Sci 119: 198–202

Martin JM, Nirel P, Thomas AJ (1987) Sequential extraction techniques: promises and problems. Mar Chem 22: 313–341

Morris JM (2005) Mechanisms and effects of light-mediated zinc uptake by photosynthetic biofilm: implications for diel metal cycling in mining-impacted streams, PhD Thesis, University of Wyoming

Morris JM, Meyer JS (2007) Photosynthetically mediated Zn removal from the water column in High Ore Creek, Montana. Water Air Soil Pollut 179(1–4):391–395

Morris JM, Nimick DA, Farag AM, Meyer JS (2005) Does biofilm contribute to diel cycling of Zn in High Ore Creek, Montana? Biogeochemistry 76:233–259

Morris JM, Farag AM, Nimick DA, Meyer JS (2006) Light-mediated Zn uptake in photosynthetic biofilm. Hydrobiologia 571:361–371

Mutz M, Rohde A (2003) Processes of surface-subsurface water exchange in a low energy sand-bed stream. Int Rev Hydrobiol 88(3–4):290–303

Nimick DA, Gammons CH, Cleasby TE, Madison JP, Skaar D, Brick CM (2003) Diel cycles in dissolved metal concentrations in streams: occurrence and possible causes. Water Resour Res 39(9). doi:10.1029/2002WR001571

Padmanabham M (1983) Comparative study of the adsorption-desorption behavior of copper(II), zinc(II), cobalt(II) and lead(II) at the goethite-solution interface. Aust J Soil Res 21:515–525

Precht E, Franke U, Polerecky L, Huettel M (2004) Oxygen dynamics in permeable sediments with wave-driven pore water exchange. Limnol Oceanogr 49(3):693–705

Quevauviller Ph, Rauret G, Griepink B (1993) Single and sequential extraction in sediments and soils. Int J Environ Anal Chem 51:231–235

Rauret G, López-Sánchez JF, Sahuquillo A, Rubio R, Davidson C, Ure A, Quevauviller Ph (1999) Improvement of the BCR three step sequential extraction procedure prior to the certification of new sediment and soil reference materials. J Environ Monit 1:57–61

Revsbech NP, Jørgensen BB (1986) Microelectrodes – their use in microbial ecology. Adv Microb Ecol 9:293–352

Riedl R, Huang N, Machan R (1972) The subtidal pump: a mechanism of intertidal water exchange by wave action. Mar Biol 13:210–221

Shaw RD, Prepas EE (1990) Groundwater lake interactions. 2. Nearshore seepage patterns and the contribution of ground-water to lakes in central Alberta. J Hydrol 119(1–4):121–136

Stein J (ed) (1973) Handbook of phycological methods. Culture methods and growth measurements. Cambridge University Press, New York, 448 pp

Strawn DG, Scheidegger AM, Sparks DL (1998) Kinetics and mechanisms of Pb(II) sorption and desorption at the aluminum oxide-water interface. Environ Sci Technol 32:2596–2601

Stumm W, Morgan JJ (1996) Aquatic chemistry. Wiley, New York, 1022 pp

Tessier A, Campbell PGC (1991) Comment on "Pitfalls of sequential extractions" by P. M. V. Nirel and F. M. M. Morel. Water Res. 24:1055–1056 (1990); Water Res 25(1): 115–117

Thibodeaux LJ, Boyle JD (1987) Bedform-generated convective transport in bottom sediment. Nature 325:341–343

Tomaselli L, Lamenti G, Tiano P (2002) Chlorophyll fluorescence for evaluating biocide treatments against phototrophic biodeteriogens. Ann Microbiol 52:197–206

Triska FJ, Duff JH, Avanzino RJ (1993) The role of water exchange between a stream channel and its hyporheic zone in nitrogen cycling at the terrestrial aquatic interface. Hydrobiologia 251(1–3):167–184

Woodruff SL, House WA, Callow ME, Leadbeater BSC (1999) The effects of biofilms on chemical processes in surficial sediments. Freshw Biol 41:73–89